Backscatter and Electromagnetic Shower Spreading in the SiD ECal

Amanda Steinhebel, James Brau
University of Oregon, Center for High Energy Physics,
1274 University of Oregon Eugene, Oregon 97403-1274 USA
(Dated: March 5, 2018)

I. OVERVIEW

The validated SiD design includes an electromagnetic calorimeter (ECal) that features twelve identical trapezoidal modules with overlapping ends that eliminate projective cracks (the darker, inner calorimeter of Fig 1). At normal incidence, the ECal contains 26 X_0 of tungsten alloy absorber for an extent of 13.9 mm beginning 1.264 m from the interaction point. More details regarding the geometry of the ECal can be found in "SiD ECal Geometry".

Photons and electrons create electromagnetic showers within the calorimeter, but a small portion of the shower is scattered off the calorimeter's edge and deflected. This is known as "backscatter". As the shower progresses through the calorimeter, its width increases due to contributions of low-energy particles leading to "shower spreading". These two effects are investigated here.

These studies were conduced with `SiD_o2_v02`, a DD4HEP-based full SiD simulation that features the overlapping geometry of the ECal. For these studies, 5000 photons of various initial energies (100, 50, 20, 10, 5, 2, and 1 GeV) were directed into the detector with $\varphi = 0$ and $\theta = \pi/2$ (at normal incidence to the ECal) with the 5 T magnetic field on. Backscatter and spreading is defined as any pixel measuring charge that is greater than 0.2 radians away from the initial particle trajectory. It was found that low-energy photon showers had a larger fraction of shower energy contained in backscatter/spreading than high-energy photon showers. Even so, no more than roughly 2.5% of the shower energy was contained within the backscatter/spreading. Backscatter and spreading could also be defined more tightly as measured charge deposits outside of 0.1 radians of the initial particle trajectory. Here, similar trends emerged related to the particle's true energy, and up to 3.12% of the shower energy was contained in the backscatter/spreading.

All figures and data files can be found at `http://pages.uoregon.edu/asteinhe/SiDNotes/backscatter/`, and the analysis scripts that create them can be found at `https://github.com/SiliconDetector/UserAnalyses/tree/master/asteinhebel_ECalAnalysis/Backscatter/`.

II. FIGURES

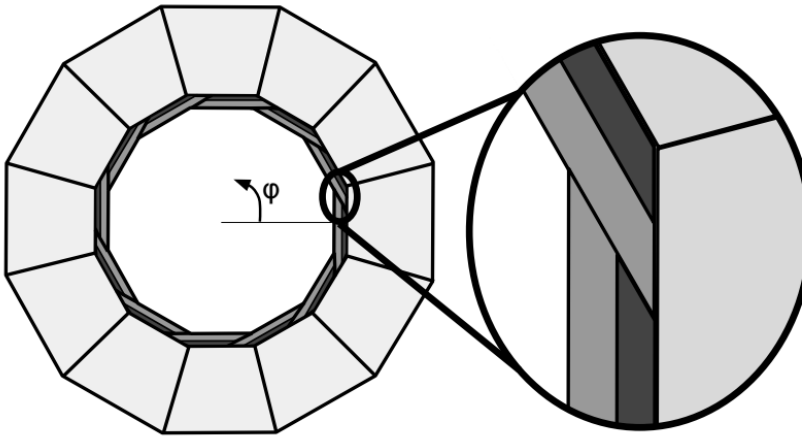

FIG. 1: Geometry of the SiD electromagnetic and hadron calorimeters. The electromagnetic calorimeter is the darker, innermost calorimeter made of twelve identical trapezoidal modules. This design creates regions where two modules overlap (shown in the cutout) to avoid projective cracks. These projective cracks can be noted in the ligher hadron calorimeter which also have twelve-fold symmetry. The two colors of the ECal indicate regions of differing absorber thickness prior to an active silicon layer. The image shows the xy plane of the detector, where the z direction is along the beamline.

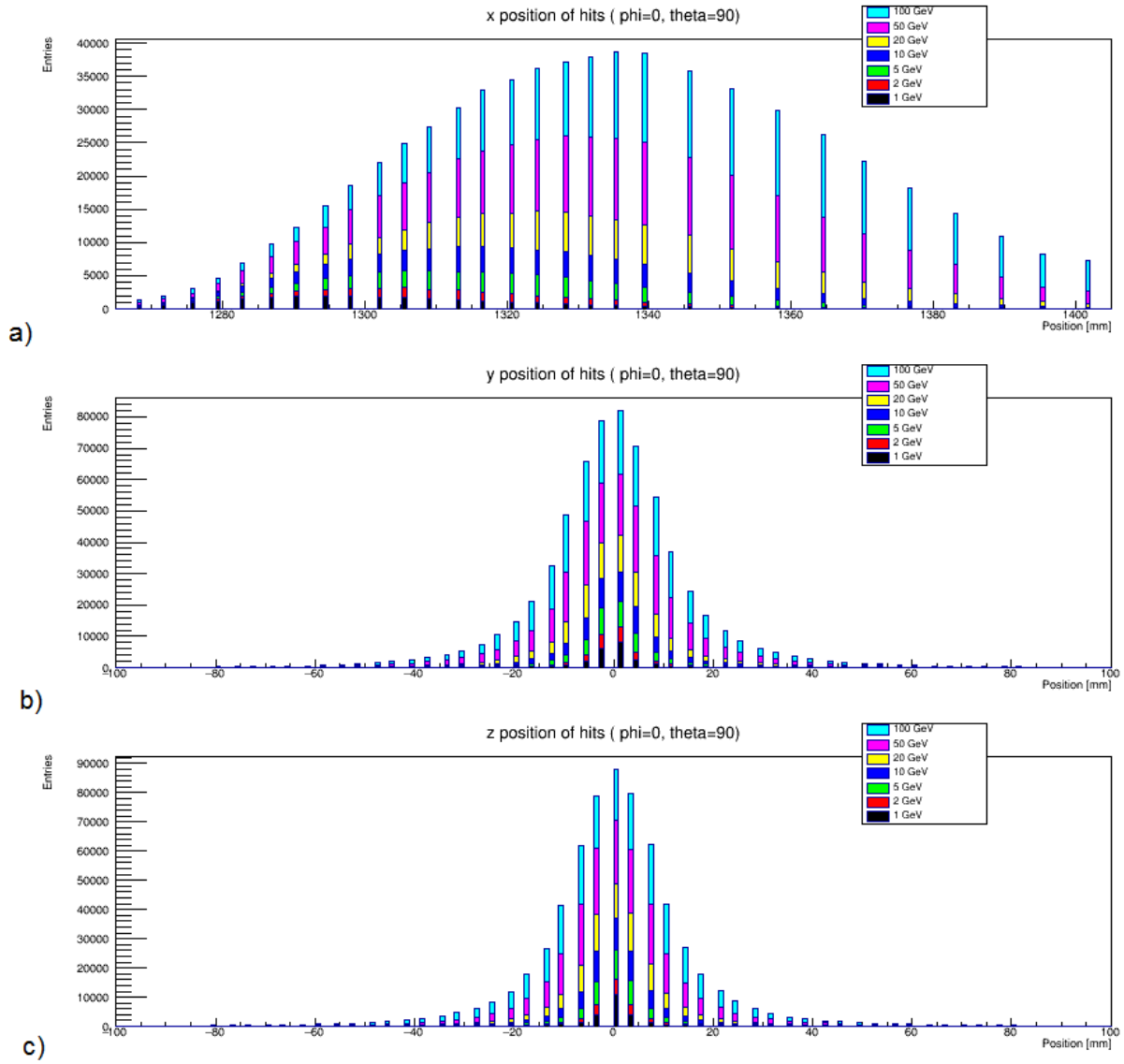

FIG. 2: The spatial components of shower distribution. At normal incidence (without the influence of the 5 T magnetic field), the shower should develop along the x direction centered at $y = z = 0$. Plots display 1 mm bins. a) shows the distribution of x positions of all hits. Positions are unequally distributed in x due to the unequal placement of active silicon layers within one module (the back ten active layers follow absorber layers that are twice as thick as those at the front of the module). Higher energy photons contain more pixels that measure a charge deposit, reach shower max deeper in the calorimeter, and may not be fully contained within the ECal alone. Lower energy incident particles reach shower max early and can be fully contained. b) and c) confirm that the shower is centered around $y = z = 0$ with a Gaussian distribution of hits around that center (indicating the shower spreading) for all energy runs.

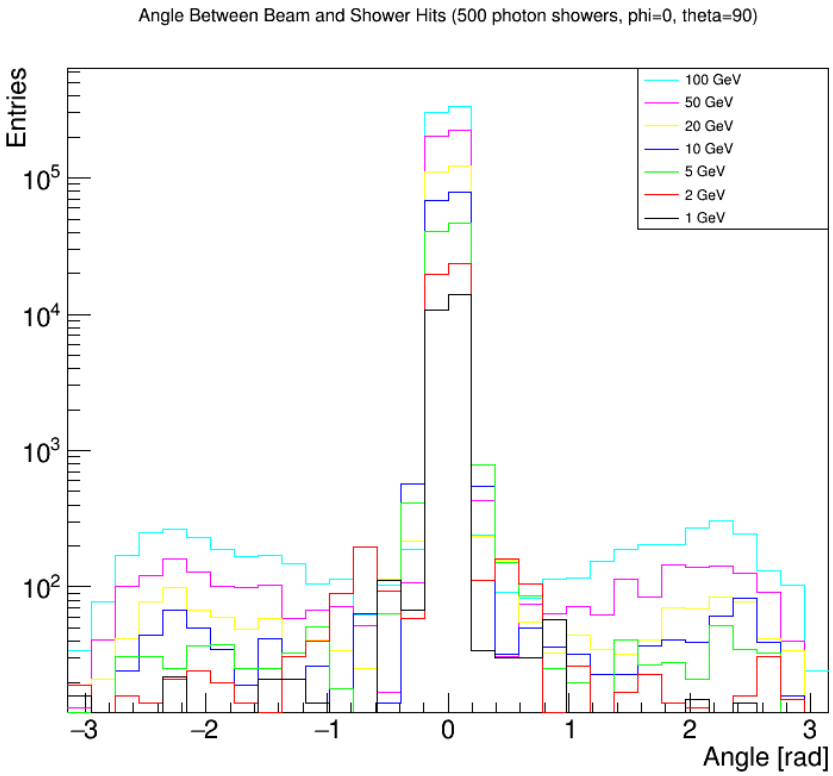

FIG. 3: The solid angle of each pixel that measured deposited charge with respect to the photon's initial trajectory along x with $y = z = 0$. For all energies, the majority of hits fall close to 0 radians away from the initial particle trajectory. The effect of backscatter at large solid angle values tends to dominate showers from high energy photons, whereas the effect of shower spreading is more pronounced relative to backscatter in the low-backscatter low energy showers. From this, cuts of 0.2 radians and 0.1 radians were considered to remove the backscattered/spread shower components.

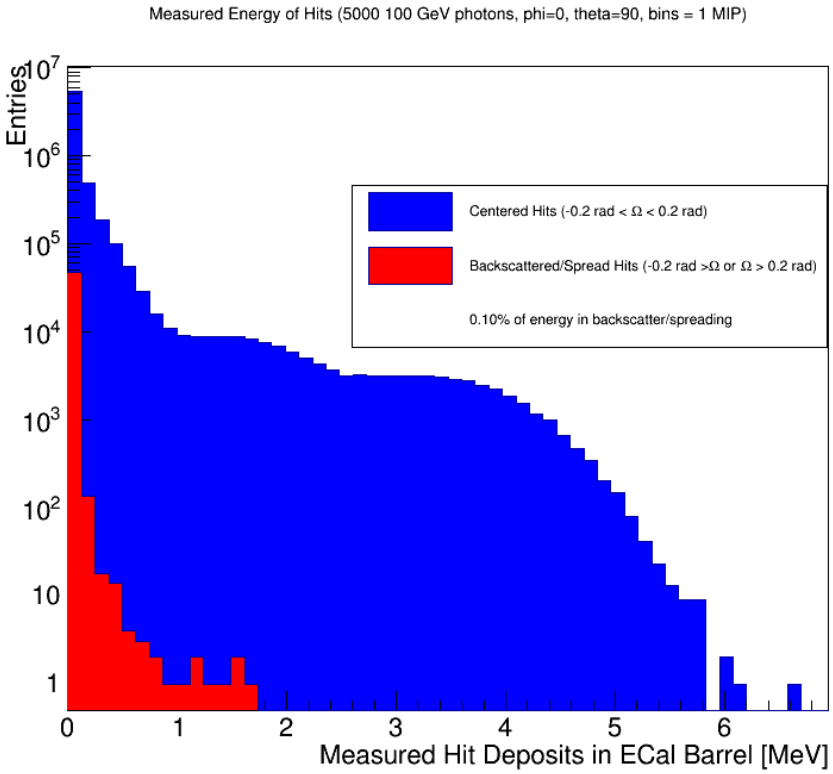

FIG. 4: The charge measured in each pixel that recorded a nonzero deposit, separated by its classification of "backscattered/spread" (red) or "centered" (blue), where backscattering/spreading is considered to occur for any solid angle greater than 0.2 radians from the initial particle trajectory. On average for the 5000 showers shown here from 100 GeV photons, 0.1% of the energy of the shower is contained within the backscatter/spreading. The following plots illustrate the same for showers resulting from incident photons over a range of energies. As the incident photon energy decreases, a larger fraction of the total shower energy is contained within the backscatter/spreading.

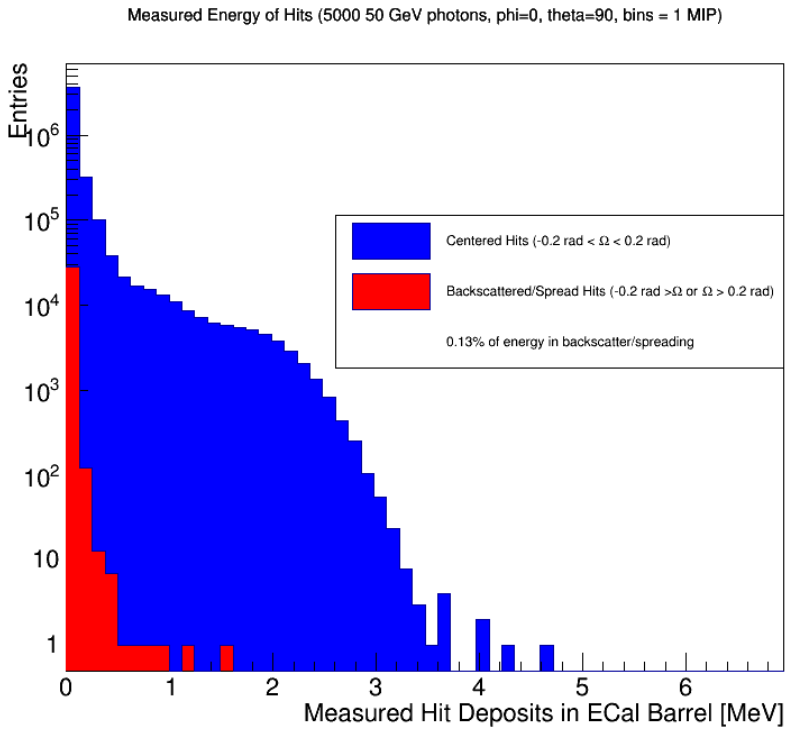

FIG. 5: 50 GeV showers. The backscatter/spreading contains 0.13% of the shower energy.

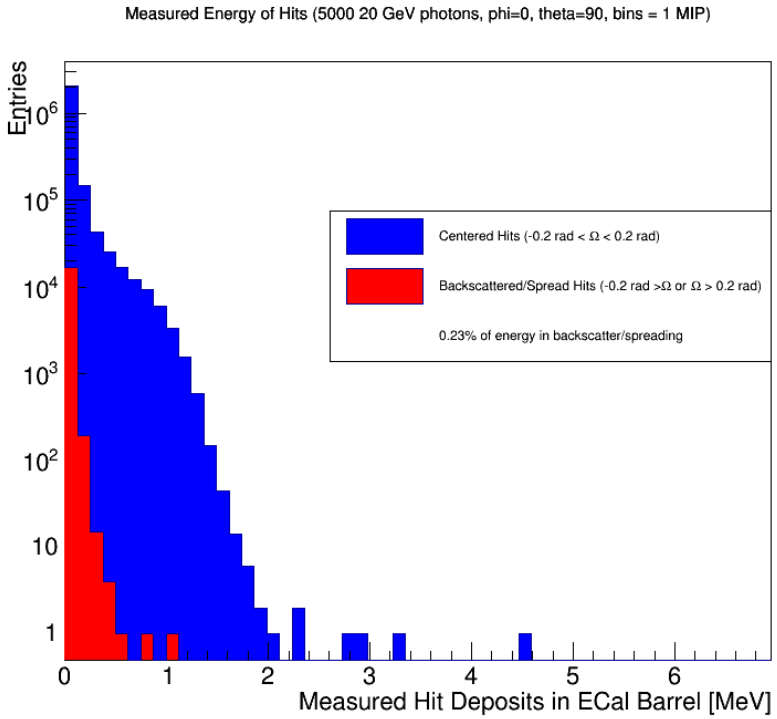

FIG. 6: 20 GeV showers. The backscatter/spreading contains 0.23% of the shower energy.

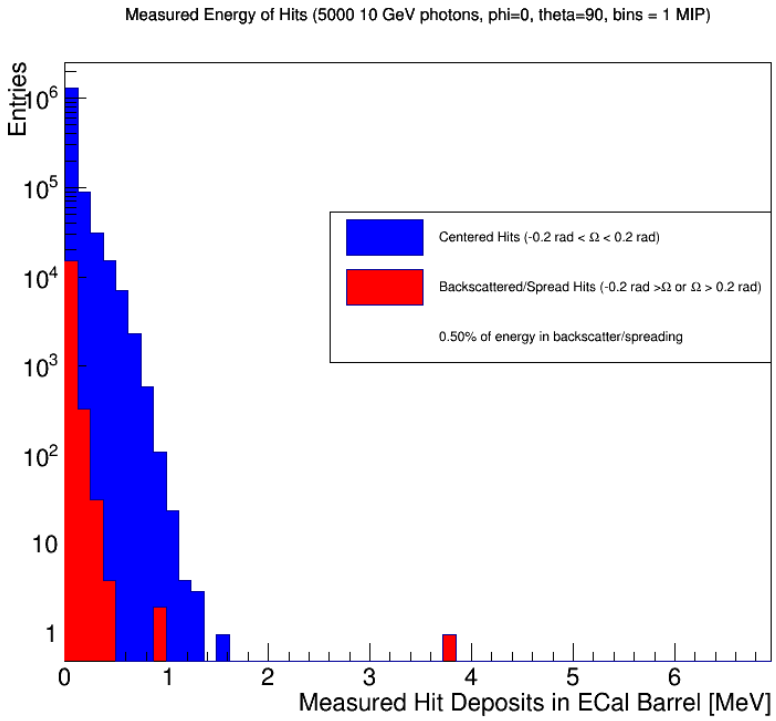

FIG. 7: 10 GeV showers.The backscatter/spreading contains 0.5% of the shower energy.

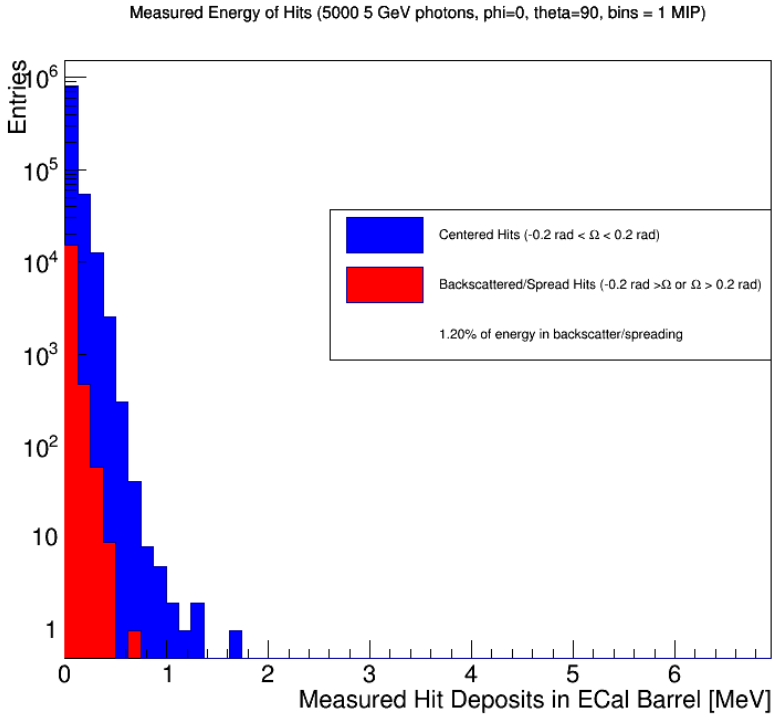

FIG. 8: 5 GeV showers. The backscatter/spreading contains 1.20% of the shower energy.

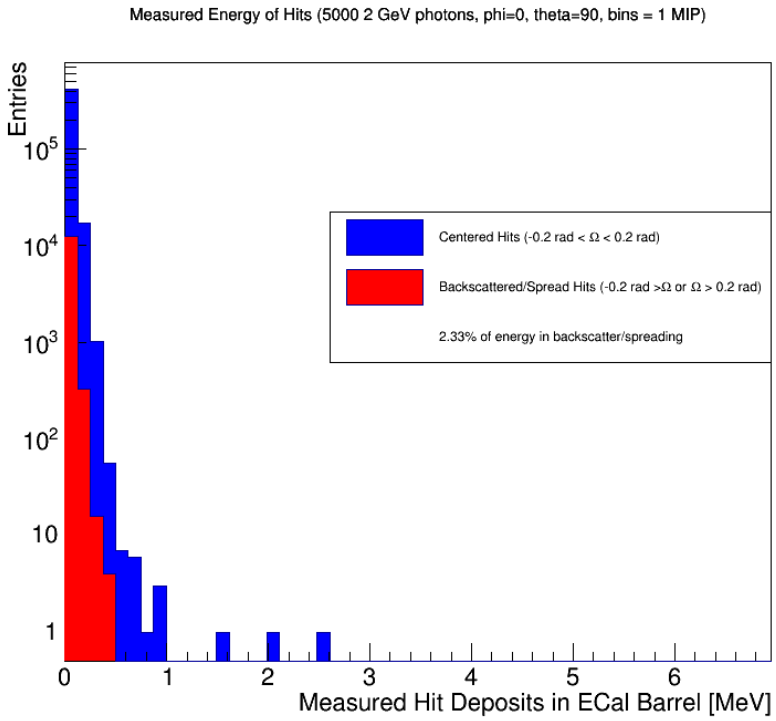

FIG. 9: 2 GeV showers. The backscatter/spreading contains 2.33% of the shower energy.

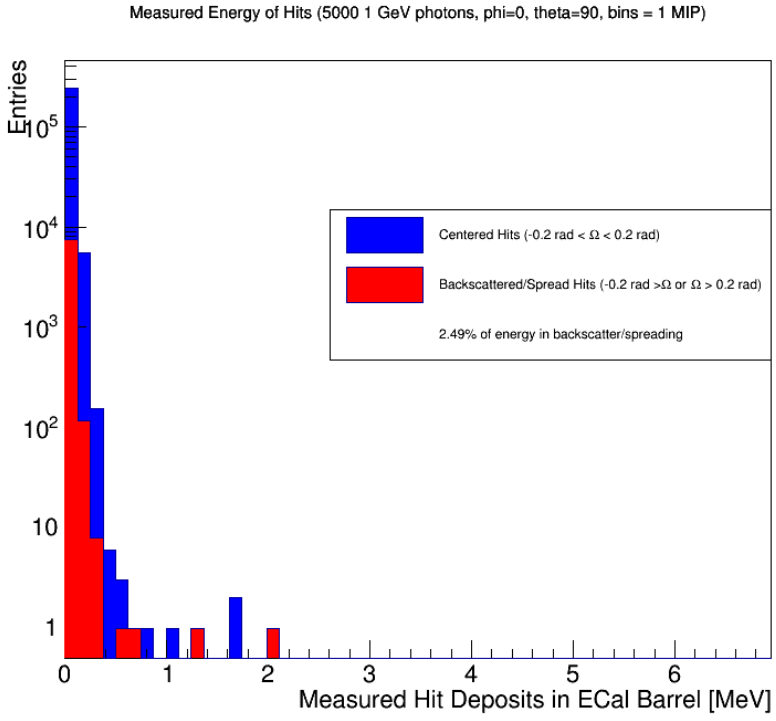

FIG. 10: 1 GeV showers. The backscatter/spreading contains 2.49% of the shower energy.

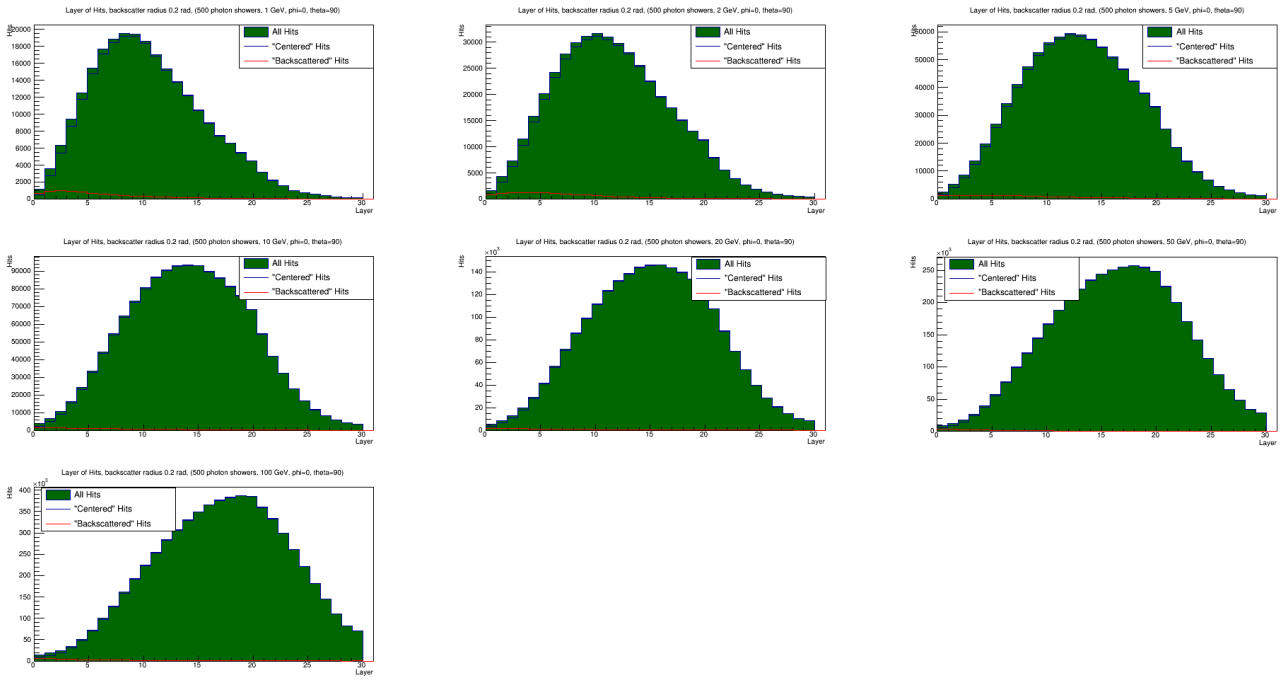

FIG. 11: The layer of each deposited charge, categorized by “centered” or “scattered/spread” with a cut on 0.2 radians. True backscatter likely deposits in the first few layers of the calorimeter, while shower spreading will be deeper (with a larger layer number). In all cases, low layer number dominate backscattered/spread deposits. The tail extends farther for low-energy showers, as shower spreading is more dominant when compared to backscatter (Fig. 3).

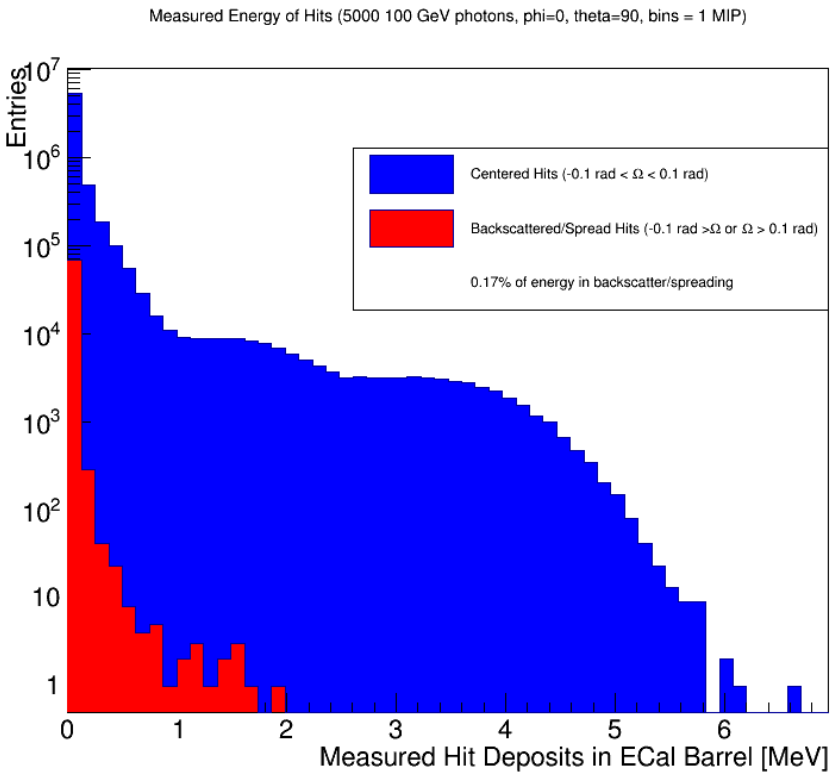

FIG. 12: The charge measured in each hit, separated by its classification of "backscattered/spread" (red) or "centered" (blue), where backscattering/spreading is considered to occur for any solid angle greater than 0.1 radians from the initial particle trajectory. On average for the 5000 showers shown here from 100 GeV photons, 0.17 % of the energy of the shower is contained within the backscatter/spreading. The following plots illustrate the same for showers resulting from incident photons over a range of energies. As the incident photon energy decreases, a larger fraction of the total shower energy is contained within the backscatter/spreading.

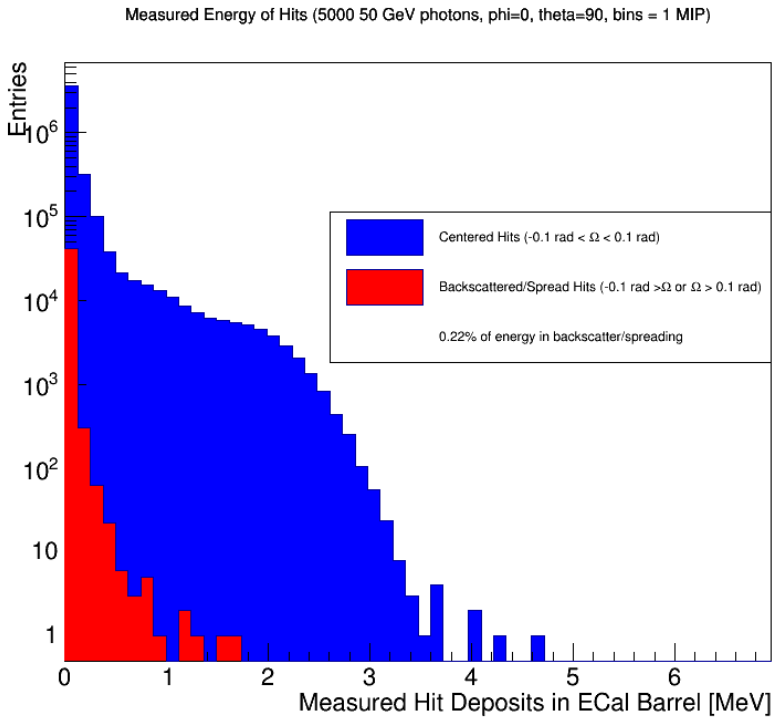

FIG. 13: 50 GeV showers. The backscatter/spreading contains 0.22% of the shower energy.

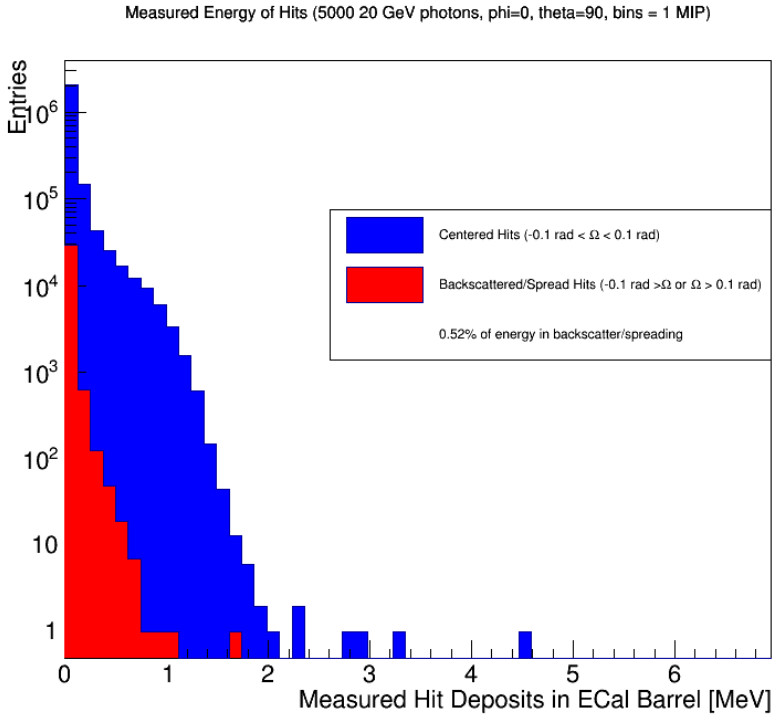

FIG. 14: 20 GeV showers. The backscatter/spreading contains 0.52% of the shower energy.

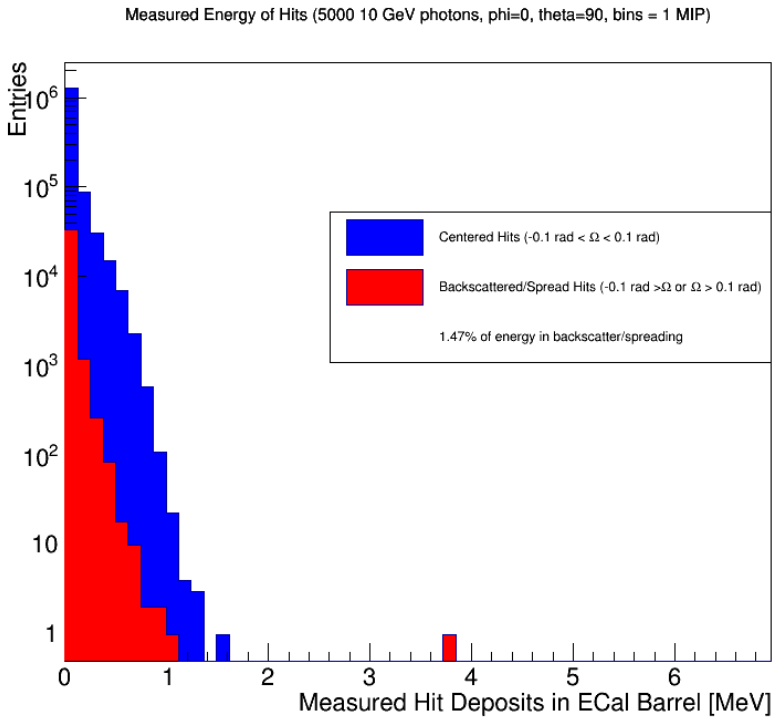

FIG. 15: 10 GeV showers. The backscatter/spreading contains 1.47% of the shower energy.

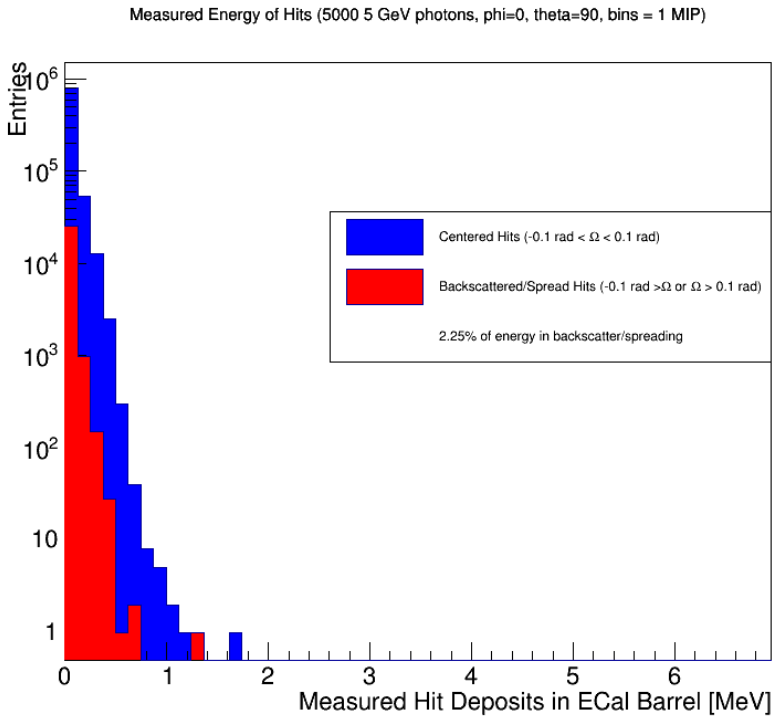

FIG. 16: 5 GeV showers. The backscatter/spreading contains 2.25% of the shower energy.

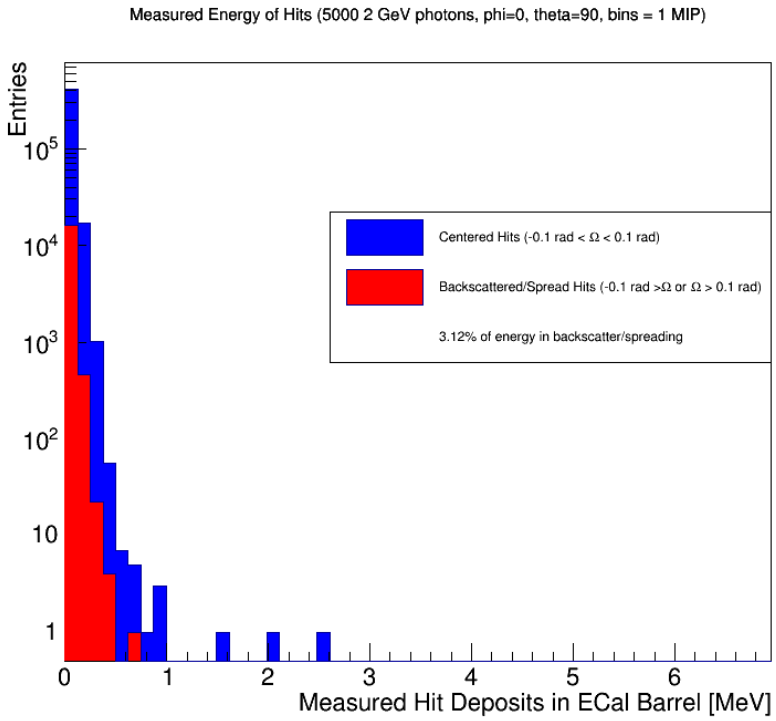

FIG. 17: 2 GeV showers. The backscatter/spreading contains 3.12% of the shower energy.

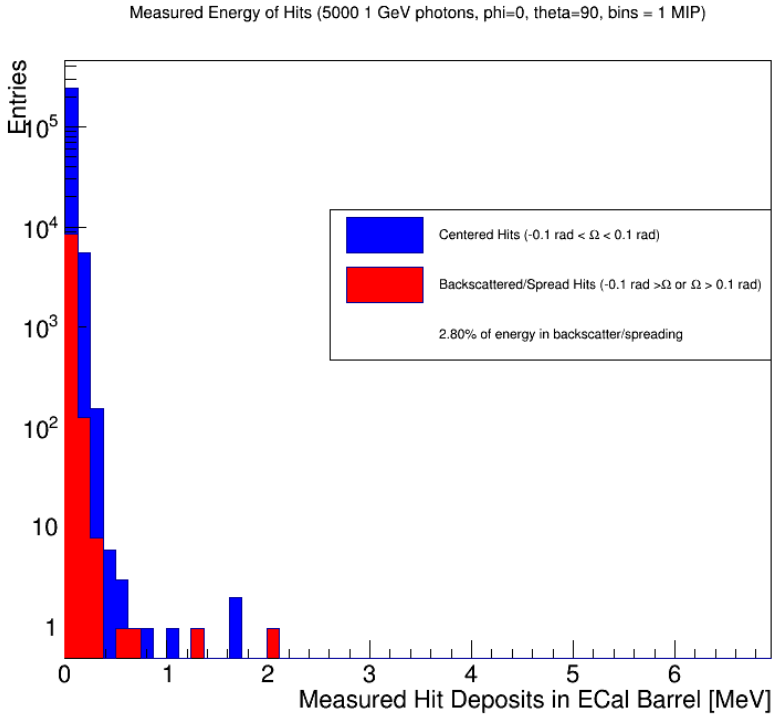

FIG. 18: 1 GeV showers. The backscatter/spreading contains 2.80% of the shower energy.

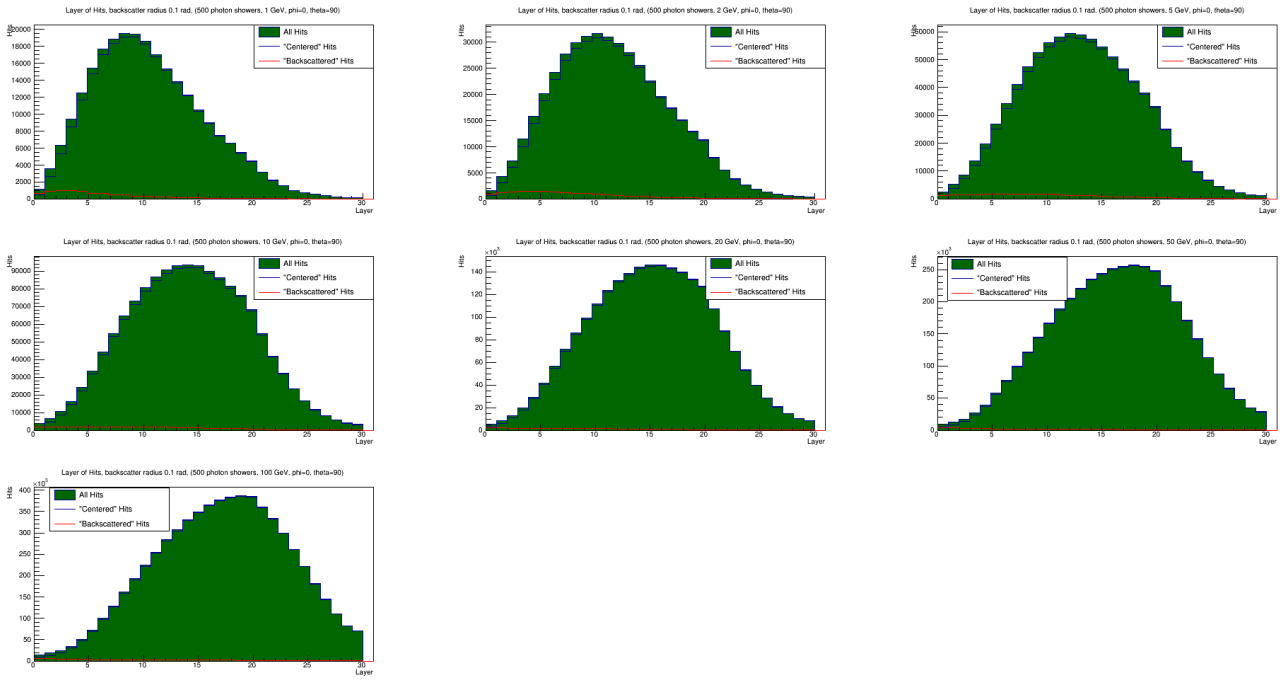

FIG. 19: The layer of each deposited charge, categorized by “centered” or “scattered/spread” with a cut on 0.1 radians. True backscatter likely deposits in the first few layers of the calorimeter, while shower spreading will be deeper (with a larger layer number). In all cases, low layer number dominate backscattered/spread deposits. The tail extends farther for low-energy showers, as shower spreading is more dominant when compared to backscatter (Fig. 3).